PROCEEDINGS OF SCIENCE

Constraining astrophysical sources of intermediate-mass ultra-high energy cosmic rays

Amadora Balladares Millalén,[a,*] **Matias Sotomayor Webar**[b] **and Neil Mark Nagar**[a]

[a] *Universidad de Concepción, Chile, Concepción*

[b] *University of Hamburg, Hamburg, Deutschland*

E-mail: aballadares2018@udec.cl, s.author@univ.country

Constraining the astrophysical source populations of Ultra High Energy Cosmic Rays (UHECRs) is difficult because UHECRs are deflected by the Galactic Magnetic Field (GMF). Recent interpretations of cosmic-ray-produced air showers with LHC-tuned hadronic interaction models suggest a gradual increase in the mean mass of UHECRs with energy. The decades-old view of UHECRs being a mix of hydrogen and iron (with relative composition varying with energy) is now expanding to also consider intermediate nuclear compositions. Notably, while hydrogen and iron UHECRs have expected mean free paths of $\sim$ 100Mpc, intermediate composition UHECRs have mean free paths of only 10s of Mpc.

Monte-Carlo simulations of H, C, N, and O composition UHECR tracks in 8 proposed GMF models can be used to estimate deflections suffered by the UHECRs detected by the Pierre Auger Observatory and the Telescope Array. These deflections can be used to identify sub-samples of 'least-deflected' UHECRs relatively independent of the GMF model assumed. The distribution of the GMF-deflection-corrected arrival directions of this 'least deflected' sample can be correlated with astrophysical catalogs to best constrain whether a substantial population of UHECRs are of intermediate composition and originate in a specific type of astrophysical source in the very local universe.

Sotomayor et al. 2022 found a strong association between the (GMF-deflection-corrected) arrival directions of 'least deflected' UHECRs with nearby (D $\leq$ 20 Mpc) galaxies when considering an oxygen UHECR composition. In this poster we present a continuation of the [1] analysis, but now using three high-abundance intermediate mass species (C, N, and O), and now weighting astrophysical samples by the fluxes, luminosities, and other properties (e.g., galaxy mass, star formation rate, radio and X-ray emission) of their galaxies.

38th International Cosmic Ray Conference (ICRC2023)
26 July - 3 August, 2023
Nagoya, Japan

*Speaker

PoS(ICRC2023)184

1. Introduction

CRs with energy higher than 10^{18}eV (1 Exa eV or EeV) are referred to as Ultra-High-Energy Cosmic Rays (UHECRs): In this study, we use UHECR to refer to those with E $\geq$ 50 EeV. The composition and sources of UHECRs, and the effect of galactic and extragalactic magnetic fields over them remain uncertain [2]. Evidence points to fully ionized nuclei that energetic astrophysical objects have accelerated to very high energies, but determining whether they are dominated by high, intermediate, or light masses remains a challenge.

The 'Hillas criterion' [3], and therefore the maximum rigidity required of the astrophysical sources, has been constantly updated that together with acceleration mechanism theory suggest that possible candidates are [4] in systems from galaxy clusters [5] to starburst superwinds [6], AGN [7], GRB jets [8]. Auger and TA have reported UHECR anisotropy ([9], [10]) and a possible correlation with AGN [11].

Recent results suggest that UHECR composition may not be only a varying mix of H and Fe. Air shower development studies ([12], [13]) and interpretation of observed data with LHC-tuned hadronic interaction models ([14], [15]) point to a gradual increase in the mean mass of UHECRs with energy and intermediate-mass UHECRs cannot be ruled out. Furthermore, Auger and TA X_{max} measurements agree that around the ankle, a light composition dominates; at higher energies, Auger found an increase in mean mass $A \approx 14 - 20$ over 40 EeV and apparently over 50 EeV there is a change in the dependence of X_{max} on E, pointing to a slow increase in mass at the highest energies.

Constraining astrophysical source populations of UHECRs is difficult since they are deflected by the Galactic Magnetic Field (GMF) so the arrival directions do not point back to the astrophysical source. While deflections by inter-galactic magnetic fields (IGMF) e.g., at the lower limit $0.01 - 0.5\mu G$; [29], are expected to be weak and disordered, Galactic magnetic fields are expected to produce significant and ordered deflections in the trajectory. Specifically, the angular deflections range from near zero to a few tens of degrees for H, increasing to hundreds of degrees for Fe. This is comparable to, or significantly larger than the error of the UHECR arrival direction determination (few degrees; e.g., [17], [18], [31], [1]).

Above $\sim 10^{19.8}$ eV there is a UHECR flux suppression due to the interactions between UHECRs and the Cosmic Microwave Background (CMB), known as the Greisen-Zatsepin-Kuzmin (GZK) effect ([20] [21]). In the intergalactic medium, UHECRs are also affected by infrared, optical, and ultraviolet (IR/OPT/UV) backgrounds, which affect the propagation of compound nuclei and the production of cosmological neutrinos, as well as by cosmological expansion, producing energy losses. The distance cutoff was estimated to be approximately 100 Mpc for proton/iron and 20 Mpc for helium/carbon/nitrogen/oxygen if $\approx$ 50% of the CRs survived [22].

We are continuing the work of [1] (e.g., Fig. 1), who found an association between the (GMF deflection-corrected) arrival directions of the 'least-deflected' UHECRs with nearby galaxies when considering an oxygen composition. Here we now use several high-abundance intermediate compositions (C, N, and O), and correlate UHECR arrival directions and GMF-deflection-corrected arrival directions with the properties of galaxies (e.g., 'fluxes' and 'luminosities' of galaxy mass, star formation rate, radio and X-ray emission) within the estimated GZK sphere of each UHECR

mass.

2. Simulations

As in [1], for calculation of the correlations of the original sources and the arrival directions, four classical models from [17] were used (AS-S, AS-A, BS-S, BS-A), three models proposed for [30] (AS-S Ring, AS-S Arm, and BS-S), and a model proposed for [31] (hereafter JF12).

The complete model of [17] consists of a spiral disk, a spiral halo component, and a dipole field. The spiral component can be modeled as axisymmetric (AS) and bisymmetric (BS). The main difference is that the AS model does not present reversals, unlike the BS. The halo component model adopted has two different parties, Symmetric (S) or Asymmetric (A) -type parity, that produce four different spiral models.
Models from [17] have a halo field component, a null vertical component because it is minimal, spatial variations of the field strength and reversals or asymmetries on the disc component, plus a random component have been introduced. Also considered is observational high-latitude rotation measures data, which constrain the model above and below the galactic plane with a toroidal magnetic field model. The galactic plane is considered with an axisymmetric magnetic field with reversals to fit observations and create a realistic model of the galactic magnetic field. The models proposed are ASS models with reversals in rings (ASS+RING), the ASS models with reversals following the arms (ASS+ARM), and a BS-S model (hereafter BS-S Sun).

The GMF model of JF12 also considers data of rotation measurements for a more realistic model. It has a halo field, a disk field, and an out-of-plane component.

The code used is a program to calculate UHECR trajectories in GMFs, started by Nagar & Matulich in 2007, and improved by [1]. We use Monte-Carlo simulations to backtrack UHECR trajectories in 8 different GMF models. Steps of 10 pc are used until the UHECR leaves a 40 kpc radius from the Galactic center; the line of sight of this last position is used as the 'out-of-galaxy', or true, arrival direction of the UHECR. The Monte Carlo simulations use uncertainties in the ordered GMF at each step, plus a turbulent component of the magnetic field. Intermediate to Fe composition UHECRs suffer significant deflections in common GMF models. The combination of disk, dipole, and halo components of a given GMF can create 'focal points or 'focal lines' in the out-of-galaxy arrival directions (see e.g., 1).

3. UHECR and Astronomical Source Samples

The sample is the same as in Sotomayor et al. 2022, but in addition to the +5.2% for PA and -5.2% for TA energy scale corrections they used, the TA and Auger energies are now additionally corrected by +10% / decade for PA and -10% / decade for TA beginning at 10 EeV following the results of the Auger-TA energy spectrum working group [28].

To correlate GMF-corrected arrival directions with candidate astronomical sources we use several relevant astronomical catalogs and the required distance cutoff of each mass composition. The catalogs are described in [1] and consist of The 105-Month Swift-BAT [27], Van Velzen radio

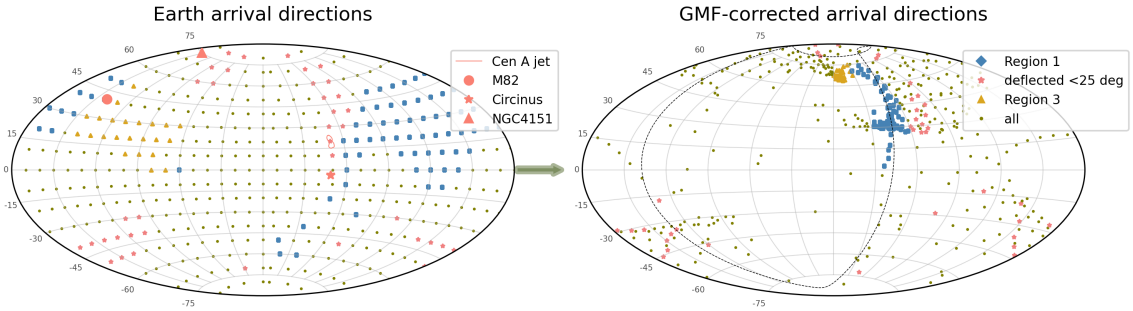

Figure 1: A simulated grid of the arrival directions of 57 EeV UHECRs (left) and their equivalent out-of-galaxy (i.e. GMF deflection corrected) arrival directions for the BSS-S GMF model and an oxygen composition. Stars (dots) denote UHECRs which suffer deflections of $\leq$ 25 ($\geq$25). To better understand the correlation between both panels, UHECRs with out-of-galaxy directions along the 'focal line' (Region 1) and 'focal point' (Region 3) are distinguished by plotting them as diamonds and triangles, respectively. Dominant sources in SFR and X-ray flux are shown in the left panel with different symbols.

galaxy [25], the Zaw optical AGN [34], the updated nearby galaxy [26], and a nearby supermassive black hole (SMBH) [35] catalog. Apart from the positions in these catalogs we also use fluxes and luminosities of the individual sources in our correlations.

We cross-matched the Karachentsev nearby galaxy catalog with the ALLWISE catalog [33] and the WISE EXTENDED SOURCE CATALOGUE (WXSC) [24], and used the WISE magnitudes to derive stellar masses following the equations of [32] and star formation rates (SFR) following the equations in [23] and [24].

4. Smoothed density maps of Astronomical Catalogs

Smoothed density maps are composed of an isotropic plus an anisotropic component. The anisotropic component was created using a Fisher function (with a specified smoothing) centered on the coordinates of the sources in each catalog, as in Abreu et al. 2010 and [11]. Each source is weighted by a relevant quantity, e.g., flux, luminosity, stellar mass, SFR. After adding the isotropic component the map is multiplied by the combined exposure map of the PAO and TA observatories, and the total function is then normalized. We do not consider a GZK suppression factor but instead, apply a distance cutoff. The final Smoothed density map can then be tested for being a proxy of UHECR flux. The Smoothed maps have a resolution of approximately 1.8°. Figures 2 and 3 show examples of such smoothed density maps (without an isotropic component) for the SFR-weighted nearby galaxy sample, and the hard-X-ray flux-weighted SWIFT-BAT AGN sample within 100 Mpc.

5. Likelihood analysis

We compare the Smoothed density maps with the arrival directions (either observed, or deflection corrected) of all (or least-deflected subsets) UHECRs detected by PAO and TA. For a given smoothed density map, and UHECR subset, the isotropic component fraction, and the smoothing of the Fisher function (sigma; which is common to all astronomical sources), are free parameters.

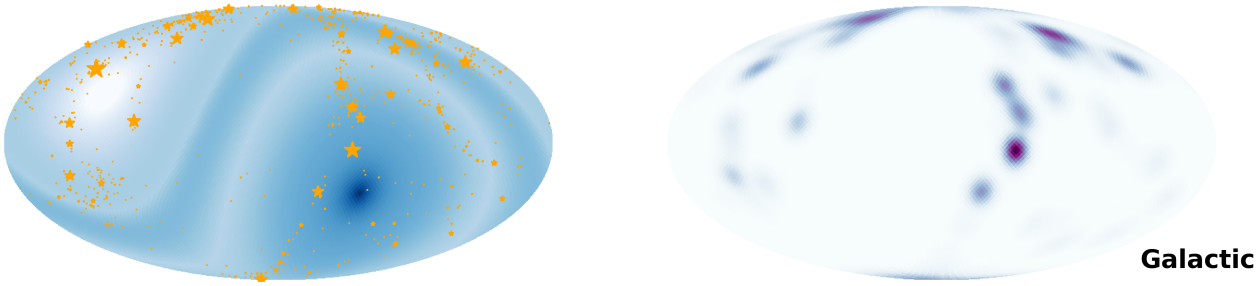

Figure 2: Left panel: Exposure map, in Galactic coordinates, of the PAO and TA observatories (with darker color indicating larger relative exposures) overplotted with galaxies from the Updated Nearby Galaxy Catalog of Karachentsev (orange stars with size proportional to their star formation rate). Right panel: the equivalent SFR-weighted map smoothed to an angular scale of 5°, weighted with the PAO and TA sky exposure map, and considering a null isotropic fraction.

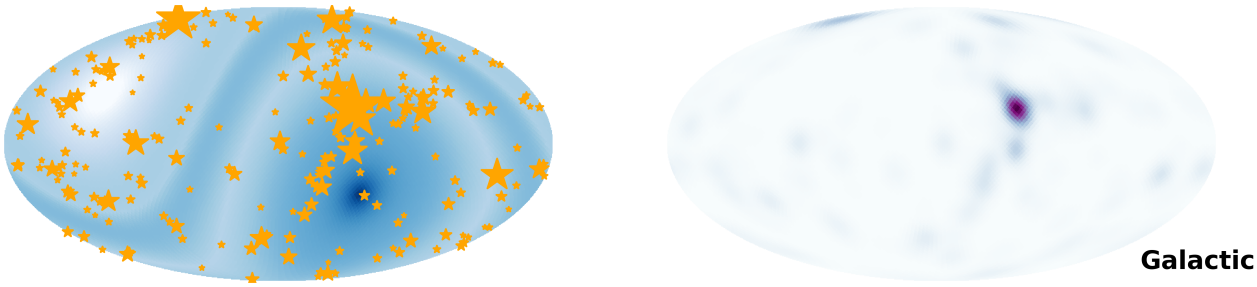

Figure 3: As in Fig. 2 but the stars in the left panel are all Seyferts, LINERs, and AGNs with D $\leq$ 100 Mpc from the SWIFT-BAT catalog, with the star size proportional to the X-ray flux.

These two values are iterated over a reasonable range (isotropic fraction from 0 to 1, and sigma from 0 to 30°) and a likelihood is determined at each iteration.

The result is the most likely smoothing and anisotropic fraction value when comparing the UHECR directions to the Smoothed map. The test statistic for deviation from isotropy is the ratio between the two nested hypotheses: the anisotropic UHECR model and the isotropic model as in [11], see Fig. 4.

Strong anisotropic correlations were observed for O, for example, with the model BS-S. But this is also due to the focal points and lines (Fig. 1) coincidentally aligned with the supergalactic plane. Thus more detailed comparisons, especially with grids, with the C and N compositions, etc., are required to clarify whether these high-test statistics are meaningful.

References

[1] Sotomayor Webar, M., Nagar, N. M., & Finlez, C. 2023, Astronomy & Astrophysics, 672, A75.

[2] Matthews, J. H. & Taylor, A. M. 2023, arXiv:2301.02682.

[3] Hillas, A. M. 1984, ARA&A, 22, 425

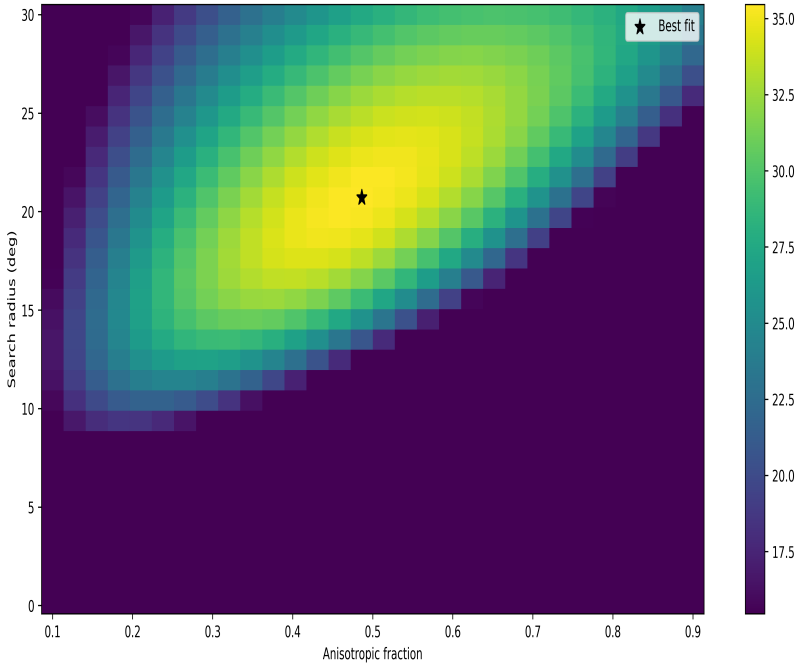

Figure 4: Test statistic profile over the search radius and the anisotropic fraction using the GMF BS-S model deflection-corrected arrival direction of all oxygen UHECRs for the SFR density map of the updated nearby galaxy catalog. The pair σ and f_{iso} that maximize the likelihood is shown with a black star.

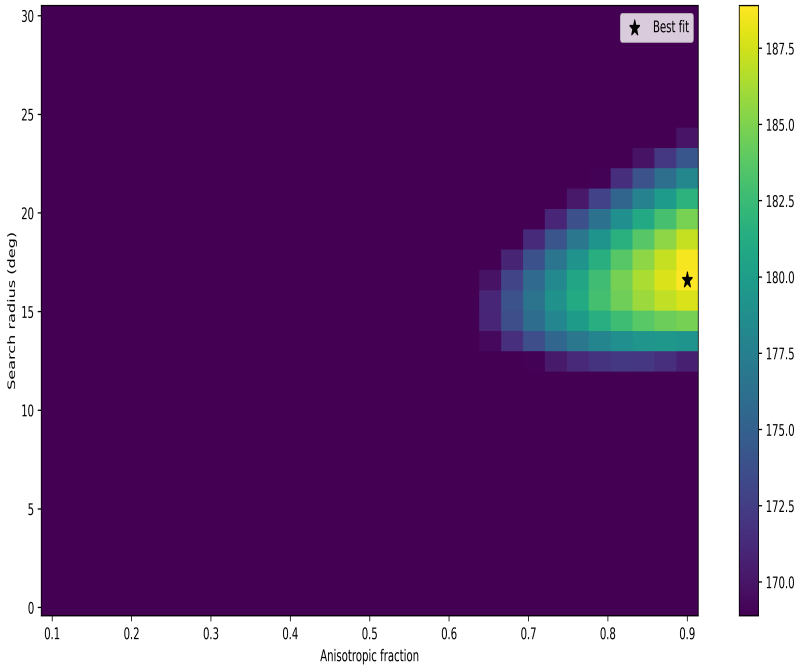

Figure 5: As in Fig. 4 using the GMF BS-S model deflection-corrected arrival direction of all oxygen UHECRs for the X-ray flux density map of nearby AGN in the Swift-BAT catalog.

[4] Blandford, R. & Eichler, D. 1987, Physics Reports, 154, 1.

[5] Kang, H., Rachen, J. P., & Biermann, P. L. 1997, Monthly Notices of the Royal Astronomical Society, 286, 257.

[6] Anchordoqui, L. A. 2018, Physical Review D, 97, 063010.

[7] Matthews, J. H., Bell, A. R., Araudo, A. T., et al. 2019, European Physical Journal Web of Conferences, 210, 04002.

[8] Globus, N., Allard, D., Mochkovitch, R., et al. 2015, Monthly Notices of the Royal Astronomical Society, 451, 751.

[9] Abbasi, R. U., Abe, M., Abu-Zayyad, T., et al. 2014, The Astrophysical Journal Letters, 790, L21.

[10] Kawata, K., Fukushima, M., Ikeda, D., et al. 2015, 34th International Cosmic Ray Conference (ICRC2015), 34, 276.

[11] Aab, A., Abreu, P., Aglietta, M., et al. 2018, The Astrophysical Journal Letters, 853, L29.

[12] Unger, M., Engel, R., Schüssler, F., et al. 2007, Astronomische Nachrichten, 328, 614.

[13] Abraham, J., Abreu, P., Aglietta, M., et al. 2010, Physical Review Letters, 104, 091101.

[14] Aab, A., Abreu, P., Aglietta, M., et al. 2014, Physical Review D, 90, 122006.

[15] The Pierre Auger Collaboration, Aab, A., Abreu, P., et al. 2017, arXiv:1710.07249.

[16] Pierre Auger Collaboration 2015, Nuclear Instruments and Methods in Physics Research A, 798, 172.

[17] Takami, H. & Sato, K. 2010, Astrophysical Journal, 724, 1456.

[18] Nagar, N. M. & Matulich, J. 2010, Astronomy & Astrophysics, 523, A49. doi:10.1051/0004-6361/200912702

[31] Jansson, R. & Farrar, G. R. 2012, Astrophysical Journal, 757, 14.

[20] Greisen, K. 1966, Physical Review Letters, 16, 748.

[21] Zatsepin, G. T. & Kuz'min, V. A. 1966, Soviet Journal of Experimental and Theoretical Physics Letters, 4, 78

[22] Kotera, K. & Olinto, A. V. 2011, Annual Review of Astronomy and Astrophysics, 49, 119.

[23] Cluver, M. E., Jarrett, T. H., Dale, D. A., et al. 2017, Astrophysical Journal, 850, 68.

[24] Jarrett, T. H., Cluver, M. E., Brown, M. J. I., et al. 2019, The Astrophysical Journal Supplement Series, 245, 25.

[25] van Velzen, S., Falcke, H., Schellart, P., et al. 2012, Astronomy & Astrophysics, 544, A18.

[26] Karachentsev, I. D., Makarov, D. I., & Kaisina, E. I. 2013, The Astronomical Journal, 145, 101.

[27] Oh, K., Koss, M., Markwardt, C. B., et al. 2018, The Astrophysical Journal Supplement Series, 235, 4.

[28] AbuZayyad, T., Deligny, O., Ikeda, D., et al. 2019, European Physical Journal Web of Conferences, 210, 01002.

[29] Vazza, F., Brüggen, M., Gheller, C., et al. 2017, Classical and Quantum Gravity, 34, 234001.

[30] Sun, X.-H. & Reich, W. 2010, Research in Astronomy and Astrophysics, 10, 1287.

[31] Jansson, R. & Farrar, G. R. 2012, Astrophysical Journal, 757, 14.

[32] Cluver, M. E., Jarrett, T. H., Hopkins, A. M., et al. 2014, Astrophysical Journal, 782, 90.

[33] Cutri, R. M., Wright, E. L., Conrow, T., et al. 2021, VizieR Online Data Catalog, II/328

[34] Zaw, I., Chen, Y.-P., & Farrar, G. R. 2019, Astrophysical Journal, 872, 134.

[35] Caramete, L. I. & Biermann, P. L. 2014, VizieR Online Data Catalog, J/A+A/521/A55